CONTROL-ORIENTED MODELLING AND CONTROL OF ROTOR VIBRATION

Zdzisław GOSIEWSKI*

* Faculty of Mechanical Engineering, Białystok Technical University, ul. Wiejska 45 C, 15-351 Białystok

gosiewski@pb.edu.pl

Abstract: Deep analysis of the control plant brings many useful information for the designer of the control system. The analysis is also important part in the design of active vibration control system. The coupling of different dynamical phenomena in rotating machinery leads to unstable vibrations. Usually, the coupling effects are caused by changing parameters. Angular speed or rotor unbalance in some applications are such parameters which change in the wide range. The problem is to find for which angular speeds we have unstable torsional/lateral vibrations. Usually, the unstable regions are in the vicinity of angular speeds where maps of natural frequencies for both dynamical systems cross each other. In the paper there was explained which intersection of torsional and lateral natural frequencies are unstable and why. The root locus method was used to explain the phenomenon. It indicated such control procedures which amplify the positive (stabilizing) mechanisms in the rotor dynamics. Such procedures can also lead to the energy saving control laws. In the case of lateral vibrations there were considered four control strategies. And these strategies were compared to indicate optimal one.

1. INTRODUCTION

The modal control of flexible structures is usually applied in analytical papers [Preumont, 2002, Ulbrich and Gunther, 2005). The modal control is a global one, while the sensors and actuators are located pointy. In control-oriented modeling it is important to find input-output relations among these points. So more, the simpler model of plant the simpler is the control design. The following disadvantages of the modal control can be noticed:

- Global approach leads to a plant model which has non-physical parameters.
- The reduction of the modal model leads to "the spillover" of the measurement and control effects.
- The control system is usually far from the optimal one from the energy point of view.
- During the control design we omit the knowledge about the plant.

The disadvantages of modal approach are particular well seen in the case of the rotor vibration control. The coupled vibrations are often met in the rotordynamics and small changes of the value of the coupling parameters can lead to the unstable behavior of the rotating machinery. So it is important to divide dynamical system into smaller subsystems and to find which parameter is responsible for the coupling of the subsystems. Such vibration analysis can indicate what one should do to design the energy saving control system.

The design procedure of the vibration control system is realized in four stages (Fig. 1a). They are: modeling of the plant and control system elements, analysis of the plant vibrations (in our case of the rotor), the design of the control law and after the implementation of the control system the experimental validation of the design procedure and dynamical behavior of the closed-loop system.

When the identification procedures were discovered (Ejkchoff, 1980; Juang, 1994) the design procedure of vibration control system can be realized in the closed loop (Fig. 1b). The experimental results can be used to identify the real rotor model. So, the improved rotor model can be again used in the next steps of the design procedure. So more, the identified model is an input-output model, so it perfectly suits the design of the control system. In the fast prototyping of the mechatronic systems we intensively apply the computer aid design methods. So, all design steps can be in practice realized parallel (Fig.1c). So more, as it was mentioned, the synthesis methods can be used to the rotor vibration analysis.

In the paper the coupling effects will be analyzed in the case of the a few-mode rotor model (similar to the Jeffcott's model (Gosiewski and Muszynska, 1992)). In the considered case we have coupled torsional/lateral vibrations which are described by three nonlinear equations. To obtain rotor motion equations one can apply the Lagrange's equations. After linearization in the inertial co-ordinate system the equations of rotor vibrations will be transformed to the system of co-ordinates which rotates together with rotor.

First, the coupling effect and its influence on the stability will be considered in the classical way (Muszynska et al., 1992). Next, we define the feedback in the coupled system and carry out investigation of the system stability with help of Evans method (root locus) known from the control theory (Kaczorek, 1993). Such approach leads to simple explanation whether given intersection on the map of natural frequencies is stable or not.

In the second part of the paper different control schemes will be used to stabilize the rotor vibrations in the wide range of the rotor angular speed. The energy effective control law will be applied to stabilize the laterarl vibrations of the rotor. We will check whether the controller also correctly stabilize the closed-loop system in the case of the torsional/lateral vibrations.

All considerations will be illustrated by the results of the computer simulations.

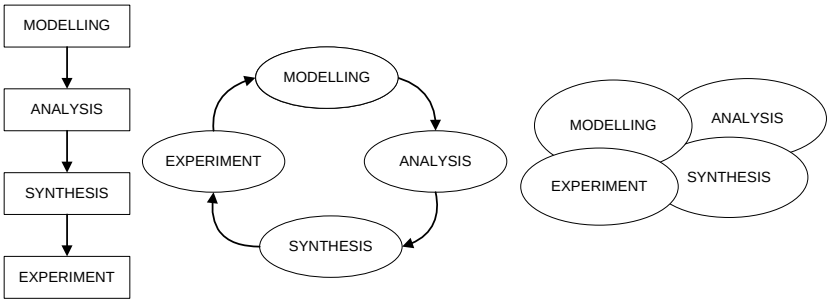

Fig. 1. Design procedure steps of the vibration control system

2. MATHEMATICAL MODEL

We consider the physical model of flexible rotor shown in Fig. 2. The model consists of a rigid disc and a massless flexible shaft. The static unbalanced disc is located in the center of the shaft. The shaft is drived by a high power motor which rotates with constant angular speed Ω. The disc has mass m and inertia momentum I_o We assume that flexibilities of the shaft in both directions: ξ, η are: k_1,k_2, respectively. The torsional flexibility coefficient is k_t.

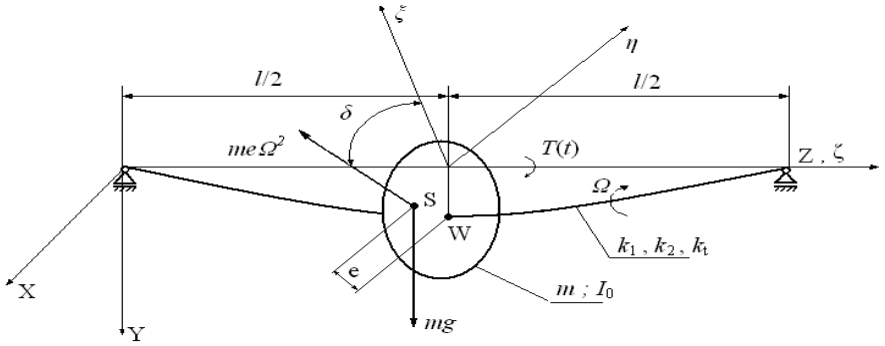

Fig. 2. Physical model of the anisotropic rotor

Kinetic energy E_k i potential energy E_p of such dynamical system are as follows:

$$E_k = \frac{m}{2}\left(\dot{x}_S^2 + \dot{y}_S^2\right) + \frac{I_O}{2}\dot{\gamma}^2 ,$$

$$E_p = \frac{k}{2}\xi^2 + \frac{k}{2}\eta^2 + \frac{k_t}{2}\left(\gamma - \Omega t\right)^2 - mgy ,$$

where: $x_s = x - e\cos(\gamma + \delta)$, $y_s = y + e\sin(\gamma + \delta)$ are coordinates of the disc mass centre S in inertial coordinate system XYZ, while: $\xi = x\cos\gamma + y\sin\gamma$, $\eta = -x\sin\gamma + y\cos\gamma$ are co-ordinates of the disc geometrical centre W in rotating co-ordinate system $\xi\eta\zeta$, which rotates with rotor angular velocity Ω. Furthermore: γ – is the angle of the shaft twist, e - is the eccentricity (distance) of rotor mass centre S from its geometrical centre W, while δ – is the angle between unbalance vector and axis ξ.

Rayleigh's function of energy dissipation in the lateral vibrations consists of two components. One component describes the dissipation caused by external vibration damping and second one describes the dissipation caused by internal damping. We assume that external damping is proportional to the rotor velocity in inertial coordinate system while internal damping is proportional to the rotor velocity in rotating coordinate system. Therefore, the Rayleigh's function is as follows:

$$E_r = \frac{1}{2}b_z\left(\dot{x}^2 + \dot{y}^2\right) + \frac{1}{2}b_w\left(\dot{\xi}^2 + \dot{\eta}^2\right) + b_t(\dot{\gamma} - \Omega)^2 =$$

$$= \frac{1}{2}b_z\left(\dot{x}^2 + \dot{y}^2\right) + \frac{1}{2}b_w\left[\left(\dot{x} + \Omega y\right)^2 + \left(\dot{y} - \Omega x\right)^2\right] + b_t(\dot{\gamma} - \Omega)^2$$

where: b_z – coefficient of external damping, b_w - coefficient of internal damping b_t - coefficient of torsional damping.

Lagrange's equations were used to obtain the motion equations of the rotor. The set of three nonlinear motion equations with periodic time-varying coefficients was obtained. So the system describes the parametric vibrations, where coefficients are a function of the rotor angular speed. To obtain the system with linear time invariant equations the non-linear equations were linearized and transformed to the rotating coordinate system (Fig.3).

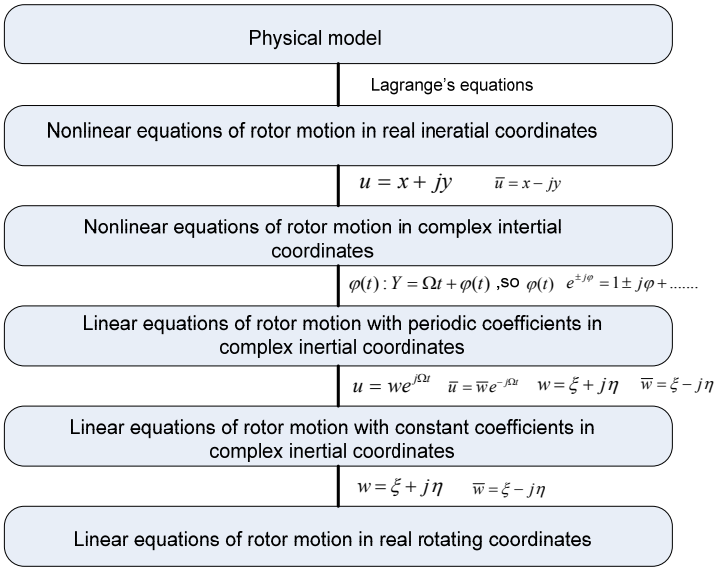

Fig. 3. Linearization and transformation of the equations describing the torsional/lateral vibrations of the rotor

The final version of the rotor model is as follows:

$$\begin{aligned}
&\ddot{\xi} - 2\Omega\dot{\eta} - \Omega^2\xi + 2h_z\left(\dot{\xi} - \Omega\eta\right) + 2h_w\dot{\xi} + \omega_1^2\xi + \\
&e\Omega^2\sin\delta\phi - 2e\Omega\cos\delta\dot{\phi} - e\sin\delta\ddot{\phi} = e\Omega^2\cos\delta + g\sin\Omega t, \\
&\ddot{\eta} + 2\Omega\dot{\xi} - \Omega^2\eta + 2h_z\left(\dot{\eta} + \Omega\xi\right) + 2h_w\dot{\eta} + \\
&\omega_2^2\eta + e\Omega^2\cos\delta\phi - 2e\Omega\sin\delta\dot{\phi} + e\cos\delta\ddot{\phi} = \\
&e\Omega^2\sin\delta + g\cos\Omega t, \\
&\ddot{\phi} + 2h_t\dot{\phi} + Rh\Omega^2\phi + \mu^2\phi + R\omega_1^2\sin\delta\xi - R\omega_2^2\cos\delta\eta = \\
&-Rg\cos\left(\Omega t + \delta\right).
\end{aligned} \tag{1}$$

where:

$$\omega_1^2 = \frac{k_1}{m}, \quad \omega_2^2 = \frac{k_2}{m}, \quad \mu^2 = \frac{k_t}{I_0}, \quad R = \frac{me}{I_0}, \quad h_t = \frac{b_t}{2I_o},$$

$$h_z = \frac{b_z}{2m}, \quad h_w = \frac{b_w}{2m}.$$

It is seen that equations are coupled by rotor unbalance ($e \neq 0$).

The linearized equations in inertial coordinates have time dependent coefficients. It means that the rotor vibrations can by considered as a parametric vibrations. From vibration theory we know that such vibrations for some range of parameters are unstable. The angular speed Ω is one of the main rotor parameters. Equations in rotating coordinates (1) have constant coefficients. Therefore, the calculations of unstable ranges of angular speed will be much simple, by the analysis of the equations in rotating coordinates.

3. FREE TORSIONAL/LATERAL ROTOR VIBRATIONS

We omit external excitations. In this case the motion equations (1) describe free rotor vibrations:

$$\begin{aligned}
&\ddot{\xi} - 2\Omega\dot{\eta} - \Omega^2\xi + 2h_z\left(\dot{\xi} - \Omega\eta\right) + 2h_w\dot{\xi} + \omega_1^2\xi + \\
&e\Omega^2\phi\sin\delta - 2e\Omega\dot{\phi}\cos\delta - e\ddot{\phi}\sin\delta = 0, \\
&\ddot{\eta} + 2\Omega\dot{\xi} - \Omega^2\eta + 2h_z\left(\dot{\eta} + \Omega\xi\right) + 2h_w\dot{\eta} + \omega_2^2\eta + \\
&e\Omega^2\cos\delta\phi - 2e\Omega\sin\delta\dot{\phi} + e\cos\delta\ddot{\phi} = 0, \\
&\ddot{\phi} + h_t\dot{\phi} + Rh\Omega^2\phi + \mu^2\phi + R\omega_1^2\sin\delta\xi - \\
&R\omega_2^2\cos\delta\eta = 0.
\end{aligned} \tag{2}$$

When we use Laplace transform the differential equations (2) will be changed to the algebraic form:

$$\begin{bmatrix} A_{1d}(s) & -B_d(s) & -D(s) \\ B_d(s) & A_{2d}(s) & -F(s) \\ -H(s) & -K(s) & C(s) \end{bmatrix} \begin{bmatrix} \xi \\ \eta \\ \phi \end{bmatrix} = \begin{bmatrix} 0 \\ 0 \\ 0 \end{bmatrix}, \tag{3}$$

where:

$$\begin{aligned}
&A_{1d}(s) = s^2 + 2(h_z + h_w)s + \omega_1^2 - \Omega^2; \\
&A_{2d}(s) = s^2 + 2(h_z + h_w)s + \omega_2^2 - \Omega^2, \\
&B_d(s) = 2\Omega(s + h_z); \\
&C(s) = s^2 + 2h_t s + eR\Omega^2 + \mu^2 \\
&D(s) = -e(\Omega^2\sin\delta - 2\Omega s\cos\delta - s^2\sin\delta); \\
&F(s) = e(\Omega^2\cos\delta + 2\Omega s\sin\delta - s^2\cos\delta); \\
&H(s) = -R\omega_2^2\sin\delta; \quad K(s) = R\omega_1^2\cos\delta.
\end{aligned} \tag{4}$$

The determinant of the main matrix in equation (3) is a characteristic polynomial. When characteristic polynomial equals zero we have characteristic equation:

$$A_{1d}(s)A_{2d}(s)C(s) - B_d(s)F(s)H(s) + D(s)B_d(s)K(s) + \\ -A_{2d}(s)D(s)H(s) - A_{1d}(s)F(s)K(s) + C(s)B_d^2(s) = 0 \quad (5)$$

When system is stable the roots (all poles) of the characteristic equation have negative real parts.

The roots have been calculated in function of rotor speed Ω for the following parameters: ω_1= 90 [rad/s], ω_2= 100 [rad/s], μ=150 [rad/s], R_h=0.01, h_z=h_w=0.04ω_1, h_t=0.02μ, ρ=30°. The results are presented in Fig. 4.

a)

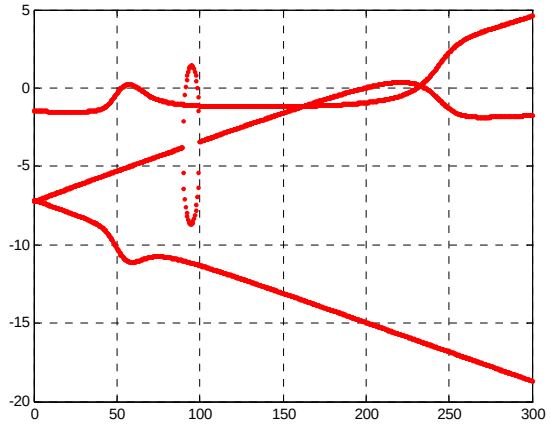

b)

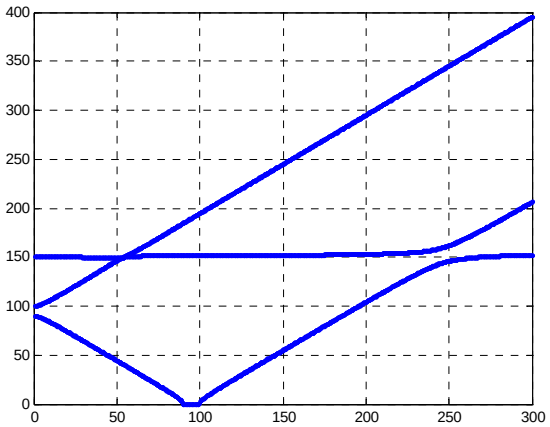

Fig. 4. Map of real part (a) and imaginary part (b) of characteristic equation roots (poles) for the torsional/lateral vibrations of the rotor with anisotropic flexibility

In the upper right quarter of the natural frequency map (Fig. 4b) we can notice three crossings of the natural frequency lines. Two crossings are in spots where torsional map meets lateral map: $\Omega \cong \mu_z - (\omega_1+\omega_2)/2$, $\Omega \cong \mu_z + (\omega_1+\omega_2)/2$. The third crossing is in the vicinity of the frequency $\Omega \cong (\omega_1+\omega_2)/2$ where the natural frequencies of lateral vibrations in two perpendicular directions ζ, η approach each other. In the vicinity of two crossings there are unstable ranges of the rotor speeds Ω.

We will show that the particular subsystems are coupled by two particular parameters: rotor unbalance R_h and rotor angular speed Ω as it is shown in Fig 5.

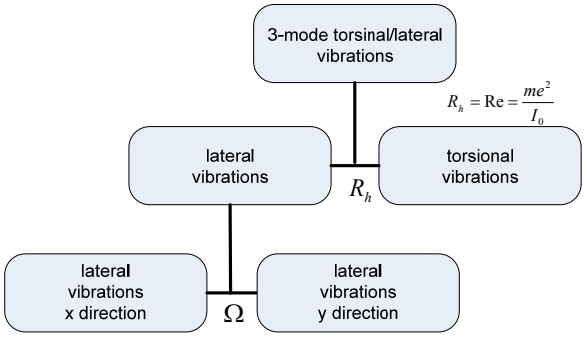

Fig. 5. Coupling parameters in considered rotor model

3.1 Undamped free vibrations of isotropic rotor

Now, we neglect the damping and assume a rotor with isotropic flexibility ω=ω_1=ω_2=100[rad/s]. In this case some of the polynomials (4) reduce to the form:

$$A = A_{1d}(s) = A_{2d}(s) = s^2 + \omega^2 - \Omega^2,$$
$$B = B_d(s) = 2\Omega s, \quad (6)$$
$$C(s) = s^2 + eR\Omega^2 + \mu^2$$

and characteristic equation can be expressed as the algebraic equation:

$$s^6 + a_1 s^4 + a_2 s^2 + a_3 = 0, \quad (7)$$

where:

$$a_1 = 2\omega^2 + 2\Omega^2 + \mu_z^2 + pR_h,$$
$$a_2 = \left(\omega^2 - \Omega^2\right)^2 + 2\left(\omega^2 + \Omega^2\right)\mu_z^2 + \omega^4 R_h + 2\Omega^2 pR_h,$$
$$a_3 = \mu_z^2\left(\omega^2 - \Omega^2\right)^2 - \omega^4 R_h + \Omega^4 pR_h,$$
$$p = \omega^2 \sin^2\delta + \omega^2 \cos^2\delta = \omega^2,$$
$$R_h = Re = \frac{me^2}{I_o}, \quad \mu_z^2 = \mu^2 + R_h\Omega^2.$$

From above coefficients of the characteristic equation it results that δ (angle between unbalance vector and axis ξ) does not influence the roots in the case of the isotropic rotor. So, we can orient the rotating coordinate system in any way against the rotor.

The stability condition is that all roots of characteristic equations have negative real parts. So using Cardan solution of the bi-3-order equation (7) we have obtained the stability conditions:

$a_3 > 0$, $a_1 > 0$,

and: (8)

$a_1^2 < 3a_2$ or $2(a_1^2 - 3a_2)^3 > [a_1(9a_2 - 2a_1^2) - 27a_3]^2$,

when: $a_1^2 > 3a_2$.

From the first inequality (8) we can calculate one of the unstable ranges of the rotor speed:

$$\omega \sqrt{\frac{\mu_z^2}{R_h \omega^2 + \mu_z^2}} < \Omega < \omega .$$

It is seen that unstable range always exists when the rotor is unbalanced ($e \neq 0$). Second inequality (8) is always fulfilled. From the third inequality (8) we have one more range of the unstable rotor speeds. Second range of the unstable rotor speeds is in the vicinity of the value: $\Omega=\omega+\mu$.

Typical maps of real and imaginary (natural frequencies) parts of the roots of characteristic equation in function of the rotor angular speed are shown in Fig. 6. The analytical considerations are confirmed by the computer simulation results. The both mentioned ranges of unstable rotor speeds are well seen in Fig.6.

a)

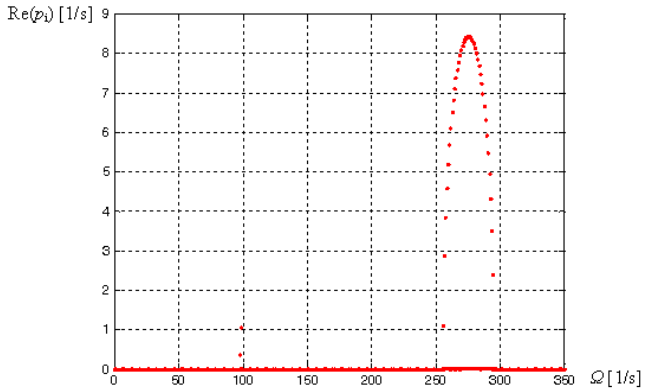

b)

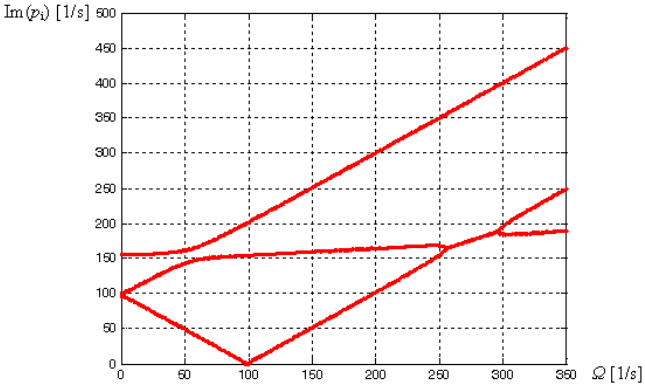

Fig. 6. Real part(a) and imaginary part (b) of characteristic polynomial roots versus rotor speed Ω for data: ω= 100 [rad/s], μ=150 [rad/s], R_h=0.1. Two ranges of unstable rotor speeds: 97 [rad/s] <Ω< 100 [rad/s], 256 [rad/s]<Ω<292 [rad/s].

The unstable speeds are in the vicinity of some natural frequency intersections (Fig. 6b). For these frequencies real part of roots have positive values (see Fig. 4a). We denote: p_i – i-th pole of transfer function (root of characteristic polynomial), z_i – i-th zero of transfer function. This time however, in comparison to Fig.4, the intersection $\Omega \cong \mu_z-(\omega_1+\omega_2)/2$ is stable while the crossing $\Omega \cong \mu_z+(\omega_1+\omega_2)/2$ is unstable. So, the problem is how to recognize which crossing indicate the unstable ranges. To answer question we will reach for a synthesis method known from the control theory.

We consider separately lateral and torsional vibrations. The coupling forces from (3) will be taken as external excitations:

$$\begin{aligned} A(s)\xi(s) - B(s)\eta(s) &= D(s)\varphi(s), \\ B(s)\xi(s) + A(s)\eta(s) &= F(s)\varphi(s), \\ C(s)\varphi(s) &= H(s)\xi(s) + K(s)\eta(s). \end{aligned} \tag{9}$$

Two first equations describe lateral vibrations and third one describes torsional vibrations. The mathematical model can be presented in the form of block scheme, given in Fig.7.

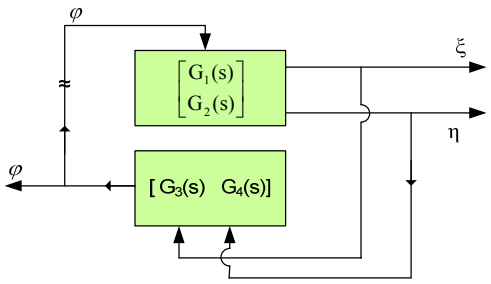

Fig. 7. Block scheme of the torsional/lateral vibrations of the flexible rotor

It is a dynamical system with feedback loop very well known from control theory, where particular transfer functions have the form:

$$\begin{aligned} G_1(s) &= \frac{\xi(s)}{\varphi(s)} = \frac{B(s)F(s) + A(s)D(s)}{A^2(s) + B^2(s)}; \\ G_2(s) &= \frac{\eta(s)}{\varphi(s)} = \frac{A(s)F(s) - B(s)D(s)}{A^2(s) + B^2(s)}; \\ G_3(s) &= \frac{\varphi(s)}{\xi(s)} = \frac{H(s)}{C(s)}; \\ G_4(s) &= \frac{\varphi(s)}{\eta(s)} = \frac{K(s)}{C(s)}. \end{aligned} \tag{10}$$

We break the feedback loop in the place indicated by tildes to obtain open-loop system. The open-loop transfer function is obtained by the multiplication of matrices:

$$G_o(s) = \begin{bmatrix} G_3(s) & G_4(s) \end{bmatrix} \begin{bmatrix} G_1(s) \\ G_2(s) \end{bmatrix} = G_3(s)G_1(s) + G_4(s)G_2(s).$$

Taking into account transfer functions (10) we have:

$$G_o(s) = \frac{H(s)B(s)F(s) + H(s)A(s)D(s) + K(s)A(s)F(s) - K(s)B(s)D(s)}{[A^2(s) + B^2(s)]C(s)}. \tag{11}$$

When we introduce the rotor parameters (4), (6) the open-loop transfer function has the form:

$$G_o(s)=\frac{-R_h\omega^2\{s^4+s^2(3\Omega^2+\omega^2)-(\omega^2-\Omega^2)\Omega^2\}}{\{s^4+2s^2(\omega^2-\Omega^2)+(\omega^2-\Omega^2)^2\}(s^2+\mu_z^2)}= \quad (12)$$

$$R_h G_r(s)$$

In the Evans method we will consider rotor unbalance parameter R_h as a gain which changes from zero to the infinity.

$$1+\frac{-R_h\omega^2\{s^4+s^2(3\Omega^2+\omega^2)-(\omega^2-\Omega^2)\Omega^2\}}{\{s^4+2s^2(\omega^2-\Omega^2)+(\omega^2-\Omega^2)^2\}(s^2+\mu_z^2)}=0$$

or (14)

$$\frac{\{s^4+2s^2(\omega^2-\Omega^2)+(\omega^2-\Omega^2)^2\}(s^2+\mu_z^2)-R_h\omega^2\{s^4+s^2(3\Omega^2+\omega^2)-(\omega^2-\Omega^2)\Omega^2\}}{\{s^4+2s^2(\omega^2-\Omega^2)+(\omega^2-\Omega^2)^2\}(s^2+\mu_z^2)}=0.$$

The numerator of the transfer function (14) is a characteristic polynomial of the closed-loop system (13) and denominator is a characteristic polynomial of the open-loop system.

$G_r(s)$ is a complex number and can be presented as a vector in the complex (Gauss) plane. According to the equation (13) the transfer function $G_r(s)$ should fulfill two conditions put on the angular location of the vector: arg $G_r(s)$=-180°±360°N, N – integer number and on its absolute value: $|G_r(s)|=1/R_h$.

From above conditions it results that for R_h increasing from zero to the infinity the open-loop poles (roots of denominator polynomial in the transfer function $G_r(s)$) move towards zeros of the same open-loop transfer function $G_r(s)$ (roots of numerator in equation (11)). If the number of poles is bigger then the number of zeros the other poles escape to the infinity along asymptotes which start from the central point in the complex plane.

It means that zeros of the open-loop transfer function should play important role in the analysis of the unbalance influence on the dynamic behavior of the coupled torsional/lateral vibrations of the flexible rotor. The real and imaginary part of transfer function zeros for rotor parameter: ω=100 [rad/s], μ=150 [rad/s], R_h=0.1 are presented in Fig 8. It is a rotor which poles (natural frequencies) are shown in Fig. 5.

As we can see in Fig. 8 the positive real parts of the zeros exist only for the rotor speed Ω range from 0 to 100 [rad/s]. Imaginary parts (frequencies) of zeros changestogether with rotor angular speed Ω and increase parallel to real parts of poles (natural frequencies) of the lateral vibrations.

For small angular speed of rotor the system can be unstable for very big values of R_h because two of zeros in transfer function $G_r(s)$ are real and positive. But value of unbalance for which it happens is unrealistic. When all zeros and poles of transfer function are purely imaginary the root locus plot moves along imaginary axis. In this case each pole has its associated zero which is a target for locus line. Two biggest poles moves to infinity along imaginary axis. Such rotor is completely stable for all values of unbalance R_h.

Now, we analyze the influence of the unbalance on the system dynamics. Closed-loop system from Fig.7 have the following characteristic equation:

$$1+R_h G_r(s)=0 \quad \text{or:}$$

$$G_r(s)=-\frac{1}{R_h},\quad \text{for } R_h\geq 0, \quad (13)$$

In our case characteristic equation of the closed-loop system has the form:

a)

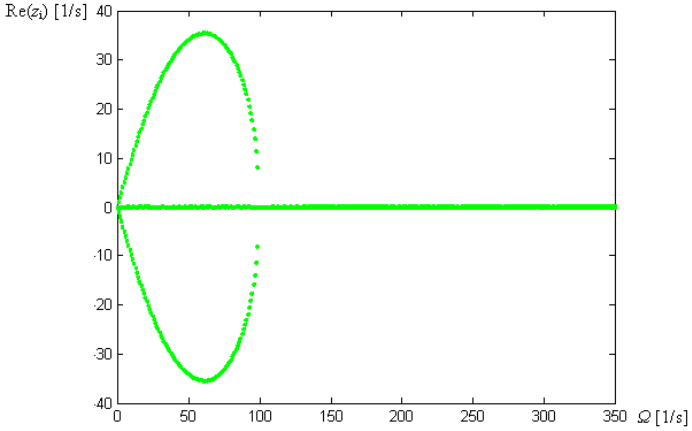

b)

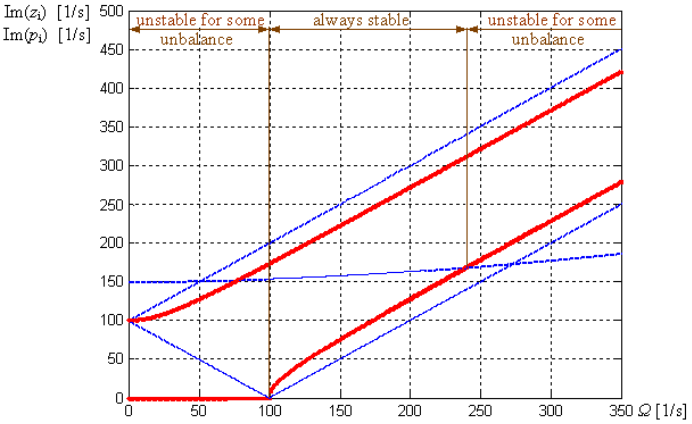

Fig. 8. The ranges of rotor speed where we can find such unbalance, which destabilize rotor vibrations Real parts (a) and imaginary parts (b) of zeros in the transfer function $G_r(S)$ versus rotor angular speed Ω drown as a bold lines. Slim lines in Fig.(b) show the natural frequencies of uncoupled torsional/lateral vibrations (poles of the transfer function $G_r(S)$).

Such harmony is destroyed when rotor angular speed cross value 245 [rad/s] (see Fig. 8). For angular speeds Ω>245[rad/s] the alteration of poles and zeros is replaced by close neighborhood of two poles. To reach open-loop zeros the locus lines are forced to make a circles. The circle enter the positive side of the complex plane. It means the motion becomes unstable for some values of unbalance.

We conclude that by analysis of the pole and zero values we are able to show the ranges of unstable vibrations (Fig.8). In first range (to 100 [rad/s]) the instability is connected with the real part positive value of two zeros of the open-loop transfer function. In second range of the unstable rotor angular speeds the alternating pole-zero pattern [Preumont, 2002] was destroyed. The neighborhood of two zeros and two poles is a simple way to detect the unstable behavior of the system. The closer to the crossing point on natural frequency map the smaller value of unbalance is needed to trigger the instability in both ranges.

3.2 Damped lateral vibrations of anisotropic rotor

Now, we will consider free damped lateral vibrations of an anisotropic rotor. To do this we reduce (3) to the following algebraic equations:

$$\begin{bmatrix} A_{1d} & -B_d \\ B_d & A_{2d} \end{bmatrix} \begin{bmatrix} \xi \\ \eta \end{bmatrix} = \begin{bmatrix} 0 \\ 0 \end{bmatrix}. \tag{15}$$

The determinant of the left matrix compared to zero is a characteristic equation:

$$\begin{aligned} &[s^2 + 2(h_z + h_w)s + \omega_1^2 - \Omega^2] \\ &[s^2 + 2(h_z + h_w)s + \omega_2^2 - \Omega^2] + 4\Omega^2 \left(s + h_z\right)^2 = 0. \end{aligned} \tag{16}$$

The roots of the characteristic equation in the function of rotor angular speed Ω are presented in Fig.9.

After some manipulations of characteristic equation (16) we can find the ranges of the unstable rotor speeds. For $\omega_1<\omega_2$ the first range is: $\sqrt{\omega_1^2 - h_z^2} < \Omega < \sqrt{\omega_2^2 - h_z^2}$.

The second range is when angular speed crosses the value: $\Omega > \left\{ \frac{h_z + h_w}{h_w} \right\} \omega_1$. The first range of unstable rotor speeds vanishes when external damping crosses the value: $h_z^2 \rangle \frac{\left(\omega_1 - \omega_2\right)^2}{8\left(\omega_1^2 + \omega_2^2\right)}$.

As it is seen in Fig.9a for both unstable ranges the real parts of some roots become positive.

a)

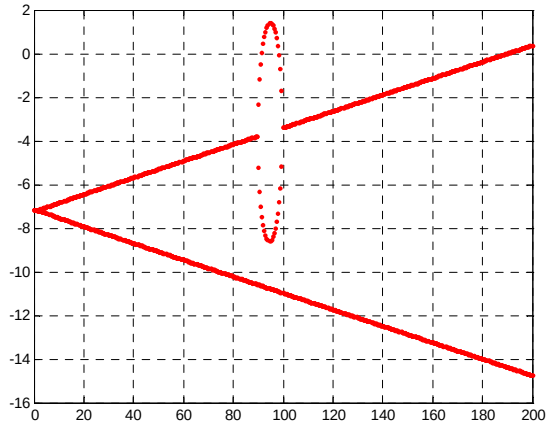

b)

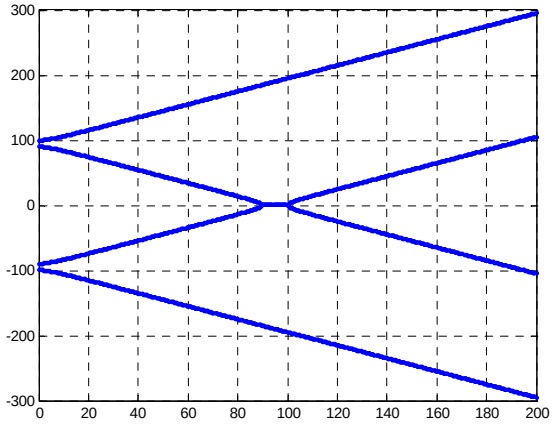

Fig. 9. Real (a) and imaginary (b) parts of the characteristic polynomial roots versus rotor angular speed Ω for lateral vibrations.

Once again we use feedback loop to decompose the system into smaller parts. We separate two perpendicular directions of the rotor lateral vibrations. The block scheme of the system is shown in Fig. 10.

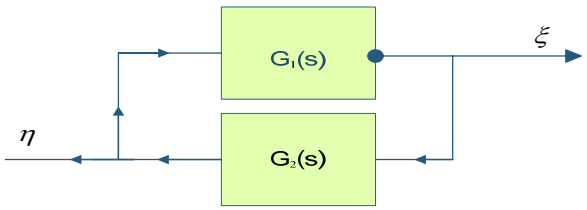

Fig. 10. The block scheme of rotor lateral vibrations

The open-loop transfer function is as follows:

$$G_{od}(s) = G_{1d}(s)G_{2d}(s), \tag{17}$$

where:

$$G_{1d}(s) = \frac{B(s)}{A_{1d}(s)}; \quad G_{2d}(s) = \frac{-B(s)}{A_{2d}(s)};$$

Finally, we have:

$$G_{od}(s) = \frac{4\Omega^2 (s + h_z)^2}{[s^2 + 2(h_z + h_w)s + \omega_1^2 - \Omega^2][s^2 + 2(h_z + h_w)s + \omega_2^2 - \Omega^2]} = R_d G_{rd}(s) \tag{18}$$

The poles of the open-loop system for different rotor speeds are presented in Fig.11. The transfer function of the open-loop system has one doubled zero and it is negative since: $z_1=z_2= -h_z$. It is evident (see Fig.11)) that open-loop system is unstable for: $\Omega>\omega_1$ while closed-loop system (Fig. 9) is stable also in the range $\omega_2<\Omega<\omega_1(h_w+h_z)/h_w$. To find mechanism which extends the range of stable rotor speeds we will again use the Evans method. According to the method some system poles will approach negative open-loop zeros while the remain ones escape along the vertical asymptotes. We assume that rotor rotation is a cause of this mechanism so we introduce an artificial Evans' gain in the form:

$$R_D = \rho 4\Omega^2 \tag{19}$$

For ρ=1 we have nominal state of the open-loop system (18). It is interesting to find for what values of the gain ρ the root locus cross the stability border on the Gauss plane.

a)

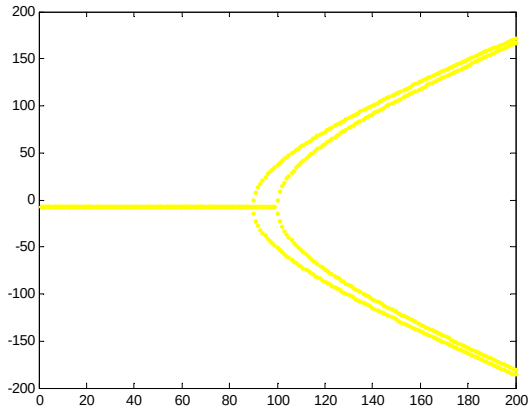

b)

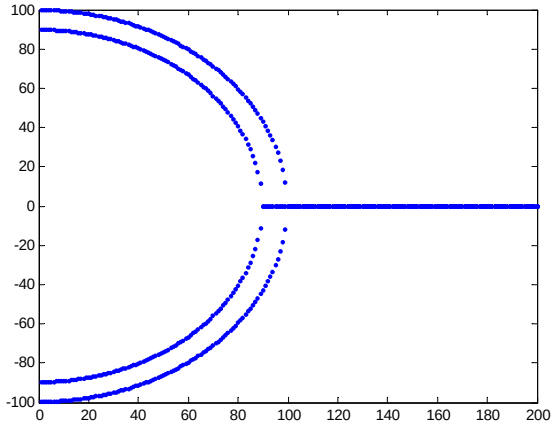

Fig. 11. Real (a) and imaginary (b) parts of the open-loop system poles versus rotor angular speed

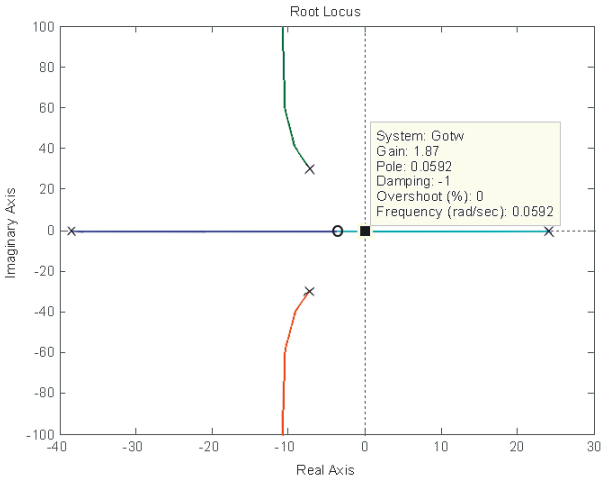

Fig. 12. Root locus of the rotor lateral vibrations in function of the gain ρ for angular speed Ω=95[rad/s]

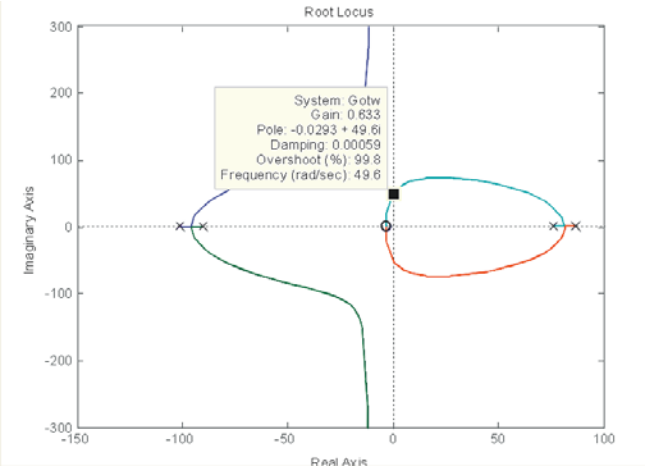

Fig. 13. Root locus of the rotor lateral vibrations in function of the gain ρ for angular speed Ω=130 [rad/s].

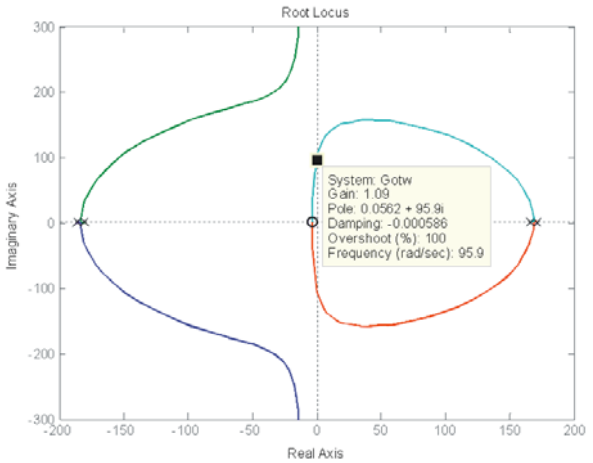

Fig. 14. Root locus of the rotor lateral vibrations in function of the gain ρ for angular speed Ω=200 [rad/s]

The root locus for unstable rotor speeds 95 [rad/s] and 200[rad/s] are presented in Fig. 12 and 14, respectively. The root locus for stable rotor speed 130[rad/s] is shown in Fig.13. The black square in Figures indicate the point on one of the root locus lines which is connected with the pole on the stability threshold. The parameters of the point are described in the Figure. For example, the overshoot on the stability border should be 100% for complex poles. The gain is the Evans gain (value of considered coupling parameter).

The imaginary axis divides the poles into stable and unstable ones. In the case of unstable rotor speeds the gain ρ crosses value 1 (ρ>1) when root locus cross the imaginary axes. It means that actual rotor speed Ω^2 is insufficient to stabilize the rotor for given speed.

3.3. Full model

Now, we return to the full model (8) whose poles are presented in Fig.2. Since now we know that zeros of open-loop system play important role in the stability analysis we have calculated them and they are presented in Fig. 15.

a)

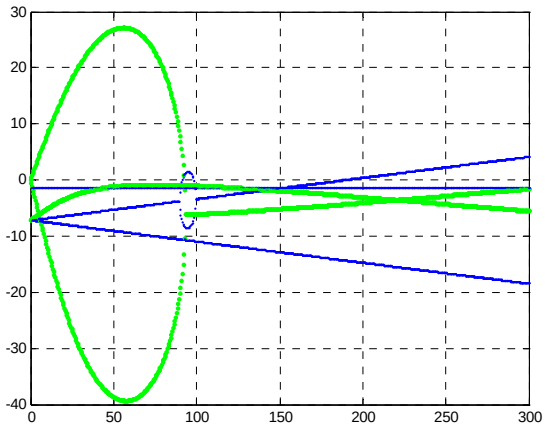

b)

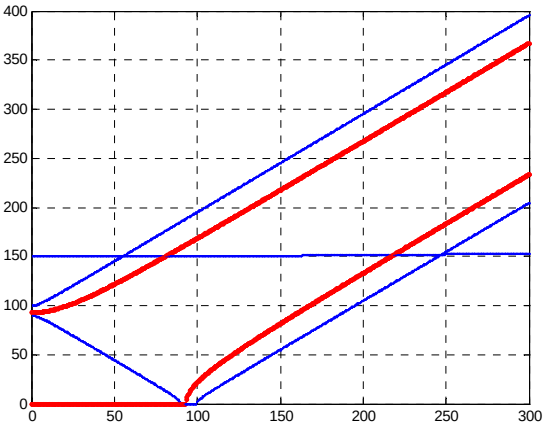

Fig. 15. Real (a) and imaginary (b) parts of zeros (bold lines) and poles (slim lines) of the open-loop transfer function designed for damped anisotropic rotor

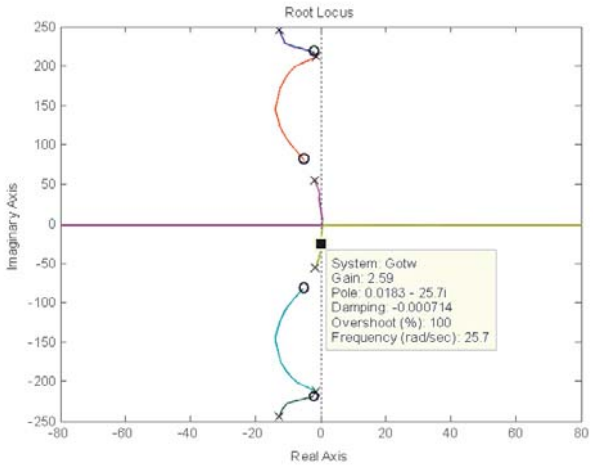

Fig. 16. Root locus for rotor angular speed Ω=150[rad/s]

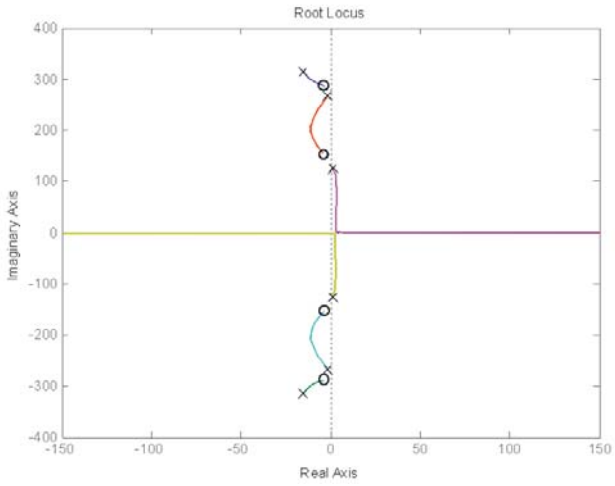

Fig. 17. Root locus for rotor angular speed Ω=220[rad/s]

We have shown in Figs 16, 17 the root locus for the two rotor speeds: 150, 220 [rad/s], respectively. In the case of Ω=150[rad/s] the rotor motion is practically stable for any unbalance. When rotor rotates with angular speed Ω=220[rad/s] the system is unstable and the unbalance practically has no influence of the dynamical state. The instability of the system is connected with internal damping.

The decomposition of coupled vibrations gives many advantages in the analysis of the system stability. The deviation of the system into smaller ones allows to reduce the calculations. It gives deeper insight into connections of the vibrations with changes of chosen parameters. Many vibration phenomena can be simply explain.

In the case of the considered torsional/lateral rotor vibrations we have carried out decoupling of the vibrations on two levels. First, we separated the torsional and lateral vibrations to analyze influence of the rotor unbalance on the rotor dynamics. Next we decoupled lateral vibrations into vibrations of the perpendicular directions. Such decomposition allowed us to show the stabilizing mechanism generated by rotor rotation.

Such approach give deeper insight into dynamical system as a control plant. Analysis of the plant dynamics allows to find the best strategy of the design procedure

of the active vibration control system. We hope that the decomposition will also be useful in the diagnostic systems.

4. CONTROL OF THE DAMPED LATERAL VIBRATIONS OF THE ANISOTROPIC ROTOR

After reanalysis of the results from section 3.2 we can improve dynamic performance of the closed-loop system (stabilization of the rotor displacement and improvement of the transient parameters) by:
- additional external damping,
- additional gyroscopic effect,
- change of system stiffness,
- active rotor balancing.

Let us consider the equations of lateral vibrations of the anisotropic rotor in form convenient to design the control law. First, the control forces are introduced to rotor movement equation (15):

$$\begin{bmatrix} A_{1d} & -B_d \\ B_d & A_{2d} \end{bmatrix} \begin{bmatrix} \xi \\ \eta \end{bmatrix} = \begin{bmatrix} f_\xi \\ f_\eta \end{bmatrix}, \tag{20}$$

where:

$$A_{1d}(s) = s^2 + 2(h_z + h_w)s + \omega_1^2 - \Omega^2;$$
$$A_{2d}(s) = s^2 + 2(h_z + h_w)s + \omega_2^2 - \Omega^2;$$
$$B_d(s) = 2\Omega(s + h_z).$$

After some calculations the relationships between control forces and rotor displacements have the form:

$$\begin{bmatrix} \xi(s) \\ \eta(s) \end{bmatrix} = \frac{1}{D_{op}} \begin{bmatrix} A_{2d}(s) & B_d(s) \\ -B_d(s) & A_{1d}(s) \end{bmatrix} \begin{bmatrix} f_\xi(s) \\ f_\eta(s) \end{bmatrix} \tag{21}$$

where:

$$D_{op} = A_{1d}(s)A_{2d}(s) + B_d^2(s) \tag{22}$$

is a characteristic polynomial of the plant.

This is the control model which has two inputs (control forces) and two outputs (measurement signals) connecting with two directions of analysed rotor vibrations: ξ, η. This relationship can be presented in matrix form as follows:

$$\mathbf{Y}_r(s) = \mathbf{G}_r(s)\mathbf{F}_r(s), \tag{23}$$

where:

$$\mathbf{Y}_r(s) = \begin{bmatrix} \xi(s) \\ \eta(s) \end{bmatrix},$$
$$\mathbf{G}_r(s) = \frac{1}{D_{op}} \begin{bmatrix} A_{2d}(s) & B_d(s) \\ -B_d(s) & A_{1d}(s) \end{bmatrix}, \tag{24}$$
$$\mathbf{F}_r(s) = \begin{bmatrix} f_\xi(s) \\ f_\eta(s) \end{bmatrix}.$$

The denominator of transfer function $\mathbf{G}(s)$ is a characteristic equation of the control plant given as follows:

$$D_{op} = (A_{1d}A_{2d} + B_d^2) = s^4 + b_3 s^3 + b_2 s^2 + b_1 s + b_0 = 0. \tag{25}$$

Where:

$$\begin{aligned} b_3 &= 4(h_z + h_w), \\ b_2 &= 4(h_z + h_w)^2 + (\omega_1^2 + \omega_2^2 + 2\Omega^2), \\ b_1 &= 2(h_z + h_w)(\omega_1^2 + \omega_2^2) + 4\Omega^2(h_z - h_w), \\ b_0 &= (\omega_1^2 - \Omega^2)(\omega_2^2 - \Omega^2) + 4\Omega^2 h_z^2 = \\ &= (\omega_2^2 - \Omega^2)^2 + 4\Omega^2 h_z^2 + (\omega_1^2 - \omega_2^2)(\omega_2^2 - \Omega^2). \end{aligned} \tag{26}$$

According to Hurwitz criterion, the open-loop system is stable if all coefficients (26) of the polynomial have the same sign (positive) and minor determinants of Hurwitz matrix are positive. As it results from equations (26) coefficients b_3, b_2 are always positive. The coefficient b_1 is positive for rotational speeds described by condition:

$$\Omega^2 < \frac{(h_z + h_w)(\omega_1^2 + \omega_2^2)}{2(h_w - h_z)}. \tag{27}$$

The condition above confirms the known phenomena - external damping increases and internal damping decreases the range of stable rotor speeds. The coefficient b_0 has two parts. The second part $4\Omega^2 h_z^2$ is always positive and the first one $(\omega_1^2-\Omega^2)(\omega_2^2-\Omega^2)$ is positive for all rotor speeds except the range:

$$\omega_1 < \Omega < \omega_2. \tag{28}$$

This unstable range of rotational speeds was earlier considered and it is a result of anisotropic rotor stiffness.

According to Hurwitz criterion in case of considered rotor system the additional two minor determinants should be positive:

$$\begin{aligned} \Delta_2 &= b_3 b_2 - b_1 > 0, \\ \Delta_3 &= b_3 b_2 b_1 - b_3^2 b_0 - b_1^2 > 0. \end{aligned} \tag{29}$$

After calculations the first minor determinant is given by:

$$\begin{aligned} \Delta_2 &= 16(h_z + h_w)^3 + 2(h_z + h_w)(\omega_1^2 + \omega_2^2) + \\ &4\Omega^2(3h_z + h_w). \end{aligned} \tag{30}$$

Thus, the minor determinant Δ_2 is positive for any rotational speed of the rotor. The stable range of rotational speeds can be calculated from condition: $\Delta_3 = b_3 b_2 b_1 - b_3^2 b_0 - b_0^2 > 0$.

It is quite difficult to calculate the condition analytically. If we assume zero damping, the condition above can be written in simpler form: $\Delta_3 = -b_0^2 > 0$. For this condition the stable range of rotational speeds is given by inequality (28).

The control forces can be written as functions of measurement signals. These relationships are called control law. Let us consider four control laws. To compare

the control laws in all control directions let introduce similary gain coefficients k. In general case, the control law can be presented as follows:

$$\mathbf{F}_r(s) = -\mathbf{K}_r(s)\mathbf{Y}_r(s). \tag{31}$$

After introducing of the control law to the equation of control plant (23) the closed-loop system is as follows:

$$[\mathbf{I} + \mathbf{G}_r(s)\mathbf{K}_r(s)]\mathbf{Y}_r(s) = \mathbf{0}, \tag{32}$$

where, the characteristic equation of the closed-loop system is given by:

$$\det[\mathbf{I} + \mathbf{G}_r(s)\mathbf{K}_r(s)] = 0. \tag{33}$$

In order to estimate the stability range of closed-loop system and to obtain the proper parameters of the controller (in our case the gain parameter k), the roots of the closed-loop characteristic equation should be analyzed.

The equation (31) describes the control law in rotational coordinate system. In practice, the rotor vibrations are controlled in non-rotating inertial coordinate system. Thus, we introduce the transformation matrix between coordinates of rotating and non-rotating coordinate systems:

$$\begin{bmatrix}\xi(t)\\ \eta(t)\end{bmatrix} = \begin{bmatrix}\sin\Omega t & \cos\Omega t\\ -\cos\Omega t & \sin\Omega t\end{bmatrix}\begin{bmatrix}x(t)\\ y(t)\end{bmatrix}, \tag{34a}$$

that is:

$$\mathbf{Y}_r(t) = \mathbf{T}\mathbf{Y}(t). \tag{34b}$$

The transformation matrix $\mathbf{T}$ is orthonormal. Thus, the inverse matrix is obtained as: $\mathbf{T}^{-1}=\mathbf{T}^T$.

The control forces (31) should also be calculated in inertial coordinate system. Thus, we also introduce the transformation matrix $\mathbf{T}$ to obtain the control forces:

$$\begin{bmatrix}f_\xi(t)\\ f_\eta(t)\end{bmatrix} = \begin{bmatrix}\sin\Omega t & \cos\Omega t\\ -\cos\Omega t & \sin\Omega t\end{bmatrix}\begin{bmatrix}f_x(t)\\ f_x(t)\end{bmatrix}, \tag{35a}$$

that is:

$$\mathbf{F}_r(t) = \mathbf{T}\mathbf{F}(t). \tag{35b}$$

After putting the formulas (34b) and (35b) into the control law (31) we obtain:

$$\mathbf{T}\mathbf{F}(t) = -\mathbf{K}_r(t)\mathbf{T}\mathbf{Y}(t) \tag{36}$$

After some calculations the control law in non-rotating coordinate system is as follows:

$$\mathbf{F}(s) = -\mathbf{K}(s)\mathbf{Y}(s), \tag{37}$$

where, the gain parameter of controller can be obtained from relation:

$$\mathbf{K}(s) = \mathbf{T}^T\mathbf{K}_r(s)\mathbf{T}. \tag{38}$$

So the control law can be calculated in rotating coordinate system (which is advantageous in case of parametric vibrations) and the last equation can be used to transform it to the inertial coordinate system.

4.1 Active damping of rotor vibrations

The damping forces are proportional to the velocity of vibrations. Let us introduce the control law where the control forces are proportional to the vibration velocity and there are no crossing couplings (see Fig. 18). Without cross couplings there are only two paths in the controller between particular control forces and rotor velocity in each of the control directions. Thus, the control law is given by formula:

$$\mathbf{F}_r(s)=\begin{bmatrix}f_\xi(s)\\ f_\eta(s)\end{bmatrix} = -k_1 s\begin{bmatrix}1 & 0\\ 0 & 1\end{bmatrix}\begin{bmatrix}\xi(s)\\ \eta(s)\end{bmatrix}. \tag{39}$$

that is:

$$\mathbf{K}_{r1}(s) = \begin{bmatrix}k_1 s & 0\\ 0 & k_1 s\end{bmatrix}. \tag{40}$$

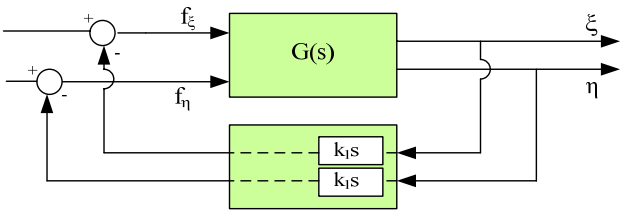

Fig. 18. The closed-loop system with the active damping f rotor vibrations

The characteristic equation of closed-loop system with control gain $\mathbf{K}_{r1}$ is given by:

$$\begin{aligned}&\det[\mathbf{I} + \mathbf{G}_r(s)\mathbf{K}_{r1}(s)] =\\ &D_{op} + k_1^2 s^2 + k_1(A_{1d} + A_{2d})s = 0.\end{aligned} \tag{41}$$

The first part of equation (41) is the characteristic equation of control plant (23). The another two parts are an appendix to the rotor dynamics introduced by the control law and the appendix has the form of the polynomial:

$$k_1^2 s^2 + k_1(A_{1d} + A_{2d})s = b_{13}s^3 + b_{12}s^2 + b_{11}s, \tag{42}$$

where:

$$\begin{aligned}b_{13} &= 2k_1,\\ b_{12} &= 4k_1(h_z + h_w) + k_1^2,\\ b_{11} &= k_1[(\omega_1^2 - \Omega^2) + (\omega_2^2 - \Omega^2)].\end{aligned} \tag{43}$$

From above results the control law influences three middle coefficients of the characteristic equation of the plant.

For the control plant with parameters: ω_1= 90 [rad/s], ω_2= 100 [rad/s], R_h=0.01, $h_z=h_w=0.04\omega_1$, we have calculated such gain coefficient k_1 of controller which brings the closed-loop system at the stability limit. These values of coefficient k_1 for different rotor angular speed Ω are called the critical coefficients. We are looking for such

control systems which stabilize rotor dynamics in given range of the rotor speeds.

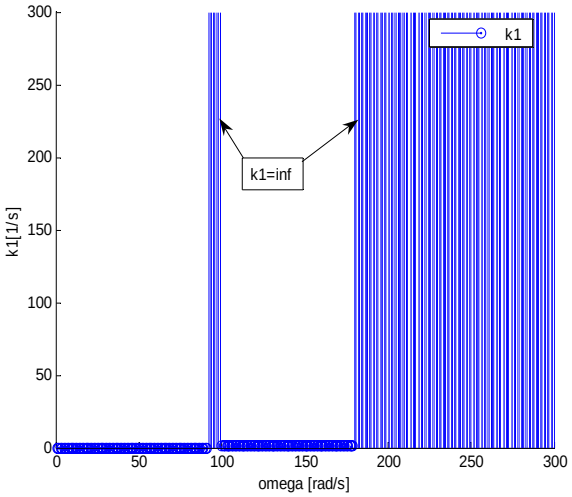

Fig. 19. Critical gain coefficients k_1 in the $\mathbf{K}_{r1}$ controller for rotor angular speed Ω from 0 to 300 [rad/s]

Unfortunately, the active control of rotor vibration damping does not ensure the stability for all rotor angular speeds (see Fig. 19). That is because the controller with gain coefficient k_1 do not influences the coefficient b_0 in the characteristic equation. Therefore, we have two unstable ranges of rotor vibrations: 92 [rad/s]<Ω<98 [rad/s] and Ω>179 [rad/s], which do not depend on controller coefficient k_1.

According to equation (38) we can control law in rotating coordinate system transform to the non-rotating coordinate system. The matrix $\mathbf{K}_{r1}$ is an identity matrix multiplied by scalar $k_1 s$. Therefore, the control law in the non-rotating coordinate system according to the equation (38) have the form:

$$\mathbf{K}_1(s) = \mathbf{T}^T \mathbf{K}_{r1}(s)\mathbf{T} = \mathbf{K}_{r1}(s). \tag{44}$$

In this case the control laws in both coordinate systems - rotating and non-rotating - are identical.

4.2. Active gyroscopic damping

The gyroscopic forces are proportional to values of rotor rotational speed. However, their direction is perpendicular to considered rotor movement. Let us introduce the control law where the control forces are perpendicular proportional to vibrations speed. There are only two feedback loops between particular control forces and rotor speeds which directions are perpendicular to directions of control forces. Thus, the control law is given by:

$$\mathbf{K}_{r2}(s) = \begin{bmatrix} 0 & -k_2 s \\ k_2 s & 0 \end{bmatrix}. \tag{45}$$

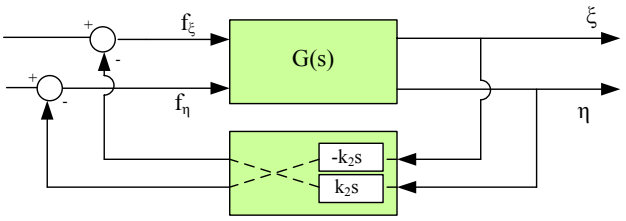

Fig. 20. The closed-loop system with the active gyroscopic damping of rotor vibrations

The characteristic equation of closed-loop system with $\mathbf{K}_{r2}$ control law is given by:

$$\det[\mathbf{I} + \mathbf{G}_r(s)\mathbf{K}_{r2}(s)] = D_{op} + k_2^2 s^2 + 2k_2 B_d s = 0. \tag{46}$$

The first part of equation (46) is the characteristic equation of control plant (21). The another two parts are introduced by
the control law of rotor dynamic and are given by:

$$k_2^2 s^2 + 2k_2 B_d s = b_{22} s^2 + b_{21} s, \tag{47}$$

where:

$$\begin{aligned} b_{22} &= 4k_2\Omega + k_2^2, \\ b_{21} &= 4k_2\Omega h_z. \end{aligned} \tag{48}$$

The control law (described above) have positive influence on the two coefficients but does not change the rest coefficients of the characteristic equation..

Unfortunately, the active gyroscopic damping of rotor vibrations does not ensure the stability for all rotational speeds (see Fig. 21). That is because the controller with gain coefficient k_2 does not influence the coefficient b_0 in the characteristic equation. Therefore, we have one unstable range of rotor vibrations: 92 [rad/s]<Ω<98 [rad/s], which does not depend of the controller coefficient k_2. For rotational speed higher than 98 [rad/s] the small value of gain coefficient k_2 is necessary to stabilize the closed-loop system. The critical value of gain coefficient k_2 increases with rotational speed Ω.

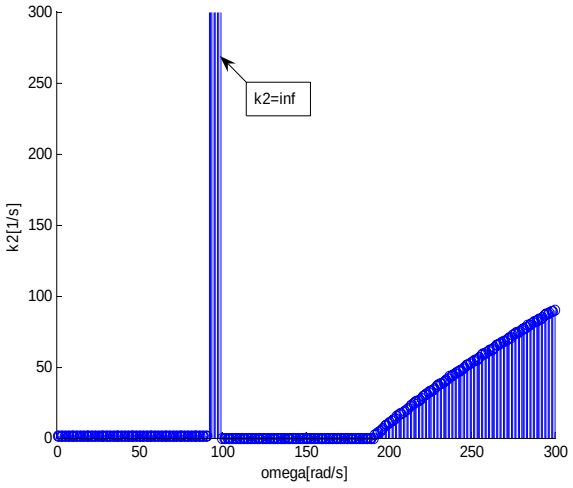

Fig. 21. Critical value of gain coefficient k_2 in the $\mathbf{K}_{r1}$ controller stabilizing the rotor vibrations for angular speeds Ω from 0 to 300 [rad/s]

Now, let us to investigate the dynamic of the closed-loop system for rotor speed Ω=300 [rad/s]. For this rotational speed the critical gain k_2 of the controller equals 91 [1/s]. The impulse response of the closed-loop rotor system in two directions of the vibrations: ξ, η for gain k_2=100 [1/s] (about 10% over critical one) is shown in Fig. 22.

The small damping of rotor vibrations in both control directions can be observed. The impulse response of the closed-loop system for gain k_2=200 [1/s] is shown in Fig. 23. The higher gain only slight improves the intensity of vibration damping.

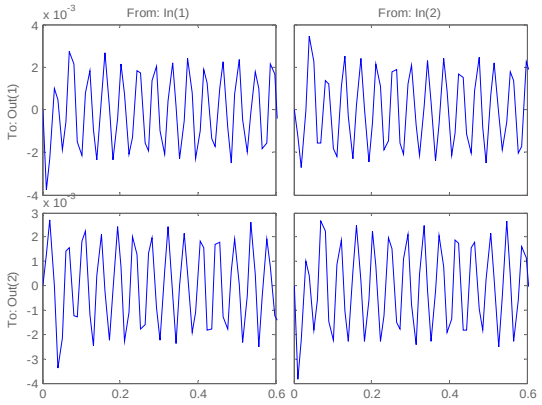

Fig. 22. The impulse response of the closed-loop system for the controller gain k_2=100 [1/s]

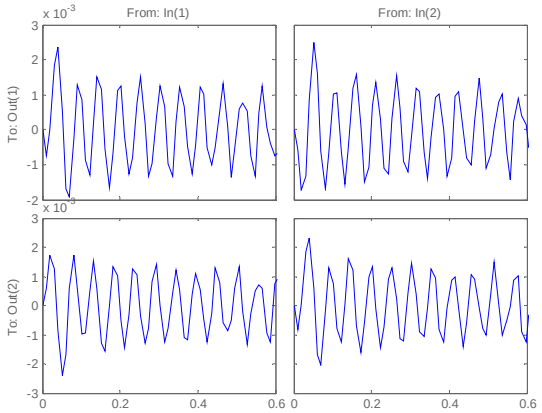

Fig. 23. The impulse response of the closed-loop for the controller gain k_2=200 [1/s]

Basing on the equation (38) we can control law transfer to the non-rotating coordinate system. The matrix $\mathbf{K}_{r2}$ is an identity matrix multiplied by scalar $k_2 s$. Therefore, in non-rotating coordinate system we have:

$$\mathbf{K}_2(s) = \mathbf{T}^T \mathbf{K}_{r2}(s)\mathbf{T} = \mathbf{K}_{r2}(s). \tag{49}$$

In this case the control laws in both coordinate systems - rotating and no rotating - are also identical.

4.3. Active change of rotor direct stiffness

According to Hurwitz criterion, all coefficients of characteristic equation of the closed-loop system should be positive. If the external damping is not big enough the last one of coefficients: $b_0=(\omega_1^2-\Omega^2)(\omega_2^2-\Omega^2)+4\Omega^2 h_z^2$ in the characteristic equation of control plant (25) is negative for the rotational speeds Ω between frequency ω_1 and ω_2. What more, any of above control laws do not change the value of coefficient b_0. Therefore, the another control law which can change the value of coefficient b_0 is necessary to be considered. The most advantageous is a control law which leads to the isotropy of the rotor system. In this case the unstable region of rotor vibrations is reduced to zero.

The stiffness forces are proportional to the displacement of rotor vibrations. Let us introduce the control law in which the control forces are proportional to the rotor displacements and there are no cross coupling. Thus, we obtain two independent feedback loops between particular control forces and rotor displacements in each of control directions (Fig.24).

The control law is given by formula:

$$\mathbf{F}_r(s)=\begin{bmatrix} f_\xi(s) \\ f_\eta(s) \end{bmatrix} = -\begin{bmatrix} k_{31} & 0 \\ 0 & k_{32} \end{bmatrix}\begin{bmatrix} \xi(s) \\ \eta(s) \end{bmatrix}. \tag{50}$$

It means:

$$\mathbf{K}_{r3}(s) = \begin{bmatrix} k_{31} & 0 \\ 0 & k_{32} \end{bmatrix}. \tag{51}$$

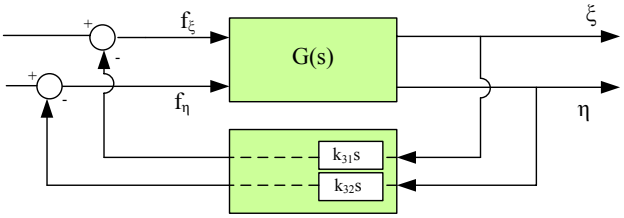

Fig. 24. The closed-loop system with controller which change the lateral system stiffness

The characteristic equation of the closed-loop system with control law $\mathbf{K}_3$ is given by:

$$\det[\mathbf{I} + \mathbf{G}_r(s)\mathbf{K}_{r3}(s)] = D_{op} + k_{31}k_{32} + k_{32}A_{1d} + k_{31}A_{2d} = 0. \tag{52}$$

The first part of equation (52) is the characteristic equation of the control plant (23). The another two parts present the influence of the controller on the closed-loop dynamics. The difference between the characteristic equation of closed-loop system and the characteristic equation of the plant is a polynomial:

$$k_{31}k_{32} + k_{32}A_{1d} + k_{31}A_{2d} = b_{32}s^2 + b_{31}s + b_{30}, \tag{53}$$

where:

$$\begin{aligned} b_{32} &= k_{31} + k_{32}, \\ b_{31} &= 2(k_{31} + k_{32})(h_z + h_w), \\ b_{30} &= k_{32}(\omega_1^2 - \Omega^2) + k_{31}(\omega_2^2 - \Omega^2) + k_{31}k_{32}. \end{aligned} \tag{54}$$

We assume first that the values of gain coefficients are the same: $k_3=k_{31}=k_{32}$. Thus, for the same values of the gain coefficients the closed-loop system is stable in full range of considered rotor angular speeds Ω (see Fig. 25).

However, the value of the critical coefficient strongly increases with the increase of the rotational speed.

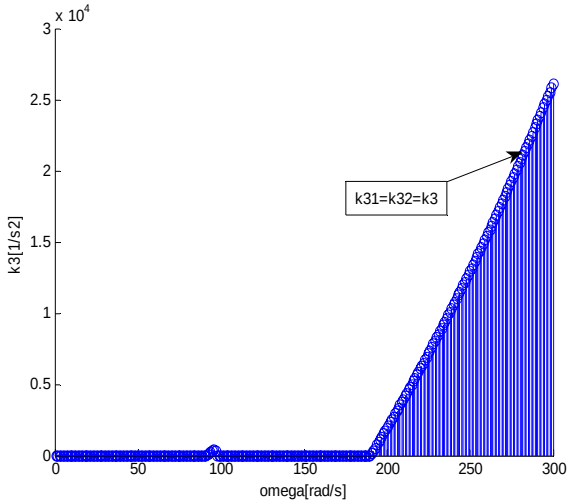

Fig. 25. The critical coefficient k_3 of $\mathbf{K}_{r3}$ controller with the same values of all gain parameters

The controller gain k_3 influences three coefficients of characteristic equation of the control plant including b_0.

Thus, the last coefficient of the characteristic equation (52) of closed-loop system is given by:

$$\begin{aligned} &b_0 + b_{30} = (\omega_1^2 - \Omega^2)(\omega_2^2 - \Omega^2) + 4\Omega^2 h_z^2 + \\ &+k_{32}(\omega_1^2 - \Omega^2) + k_{31}(\omega_2^2 - \Omega^2) + k_{31}k_{32} = \\ &= (\omega_1^2 + k_{31} - \Omega^2)(\omega_2^2 - \Omega^2) + \\ &4\Omega^2 h_z^2 + k_{32}(\omega_1^2 - \Omega^2) + k_{31}k_{32}. \end{aligned} \tag{55}$$

If we assume:

$$\begin{aligned} &k_{32} = 0, \\ &\omega_1^2 + k_{31} = \omega_2^2, \end{aligned} \tag{56}$$

the closed-loop system with rotating rotor is stable and isotropic.

In this case the gain matrix of the controller (51) in rotating coordinate system has different elements. Thus, the gain matrix of controller in non-rotating coordinate system basing on the transformation (38) has the form:

$$\mathbf{K}_3(s) = \mathbf{T}^T \mathbf{K}_{r3}(s)\mathbf{T} = \begin{bmatrix} k_{31}\sin^2\Omega t + k_{32}\cos^2\Omega t & k_{31}\sin\Omega t\cos\Omega t - k_{32}\sin\Omega t\cos\Omega t \\ k_{31}\sin\Omega t\cos\Omega t - k_{32}\sin\Omega t\cos\Omega t & k_{32}\sin^2\Omega t + k_{31}\cos^2\Omega t \end{bmatrix}. \tag{57}$$

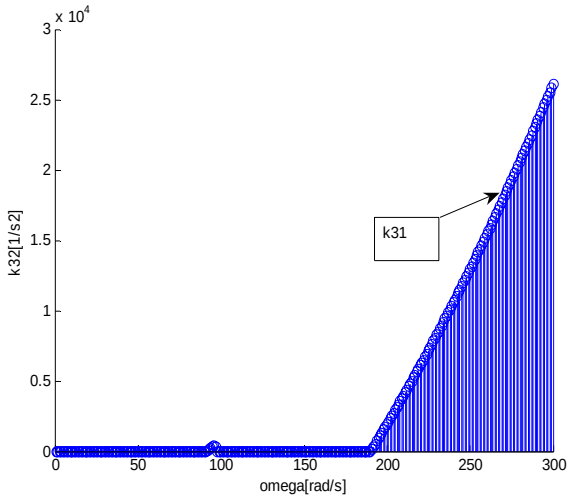

Fig. 26. The critical gain coefficient k_{31} of $\mathbf{K}_{r3}$ controller when gain parameter k_{32}=0

When we assume in (57) that k_{32}=0, we obtain the control law in inertial coordinate system given by:

$$\mathbf{K}_3(s) = \begin{bmatrix} k_{31}\sin^2\Omega t & k_{31}\sin\Omega t\cos\Omega t \\ k_{31}\sin\Omega t\cos\Omega t & k_{31}\cos^2\Omega t \end{bmatrix}. \tag{58}$$

The control law (58) means that two control inputs and two measurement output must be used to ensure the rotor isotropic stiffness.

Let us check the case when gain coefficient k_{32}=0. Now, we try to find a value of the gain k_{31} for which the SISO closed-loop system is stable. This situation is presented in Fig. 26. It is the same as is Fig. 25. where both gain coefficients had the same value. That means, we can apply the SISO control system and obtain the same results as in two input-two output control. However, the SISO control in rotating coordinate system must be transformed to two input-two output control system in non-rotoating coordinate system (see equation 58). Therefore, it is more convenient to apply two input-two output control with the same gains in order to avoid time-variant gain parameters in the $\mathbf{K}_3$ controller.

4.4 Active change of cross symmetry stiffness

Now, we consider the control law where the control forces are proportional to rotor displacements in the cross configuration. Thus, we obtain two feedback loops between particular control forces and rotor displacements which directions are perpendicular to directions of control forces (see Fig. 27). The control law is given by:

$$\mathbf{K}_{r4}(s) = \begin{bmatrix} 0 & -k_4 \\ k_4 & 0 \end{bmatrix}. \tag{59}$$

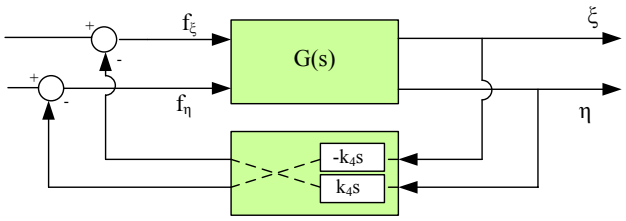

Fig. 27. The closed-loop system with controller which change the lateral stiffness in cross configuration of the rotor system

The characteristic equation of the closed-loop system with control gain $\mathbf{K}_4$ is given as follows:

$$\det[\mathbf{I} + \mathbf{G}_r(s)\mathbf{K}_{r4}(s)] = D_{op} + 2B_d k_4 + k_4^2 = 0. \quad (60)$$

The two last parts of equation (60) present influence of the control law onto rotor dynamics:

$$2B_d k_4 + k_4 = b_{41}s + b_{40}, \quad (61)$$

where:

$$b_{41} = 4\Omega k_4, \qquad b_{40} = 4\Omega k_4 h_z + k_4^2. \quad (62)$$

This control law (described above) has positive influence on the dynamics of the closed-loop. For any values of angular speed this control law increases the value of coefficients b_1 and b_0 which represent the negative effects of the internal damping and of the rotor anisotropic stiffness.

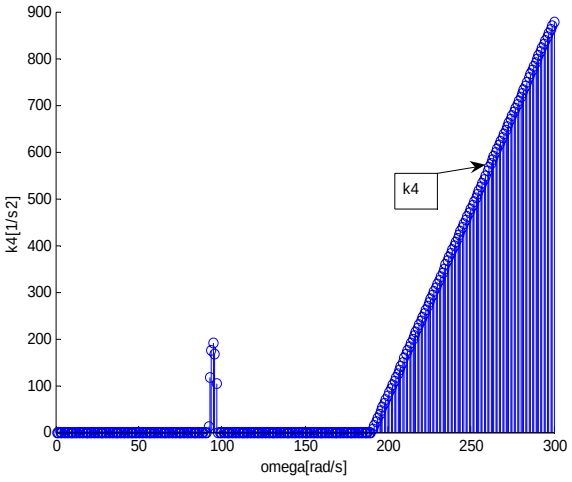

Fig. 28. The critical gain parameter k_4 in $\mathbf{K}_{r4}$ controller versus the angular speed Ω

The critical value of gain k_4 was presented in the Fig. 28. The cross change of system stiffness by $\mathbf{K}_{r4}$ controller require significantly reduces the critical gains in the comparison with the $\mathbf{K}_{r3}$ controller.

Therefore, we check dynamical behaviour of closed-loop system for rotational speed Ω=300[rad/s]. For this rotational speed the critical gain parameter is k_4=900 [1/s]. First, we apply the gain parameter k_4=1000[1/s^2] (about 10% over the critical one). The impulse responses of the closed-loop system in two vibration directions: ξ, η for critical gain parameter k_4=1000 [1/s] are shown in Fig. 29.

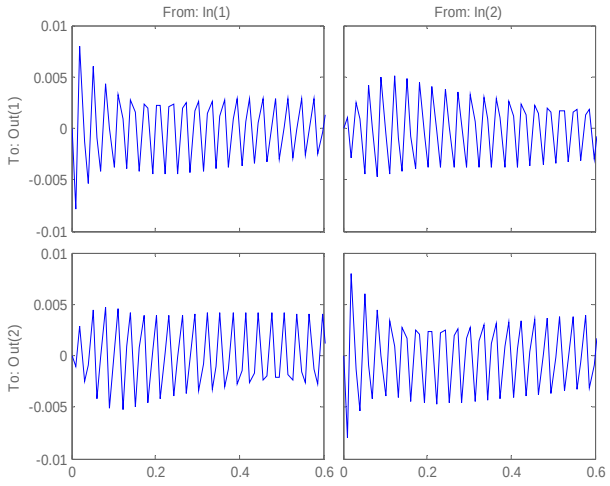

Fig. 29. The impulse response of closed-loop system for cross symmetric $\mathbf{K}_{r4}$ controller with gain k_4=1000 [1/s]

In above case we can observe small damping of rotor vibrations in both control directions. In the next step we increase the gain of the controller. The impulse responses of closed-loop system for gain controller k_4=1500 [1/s] atr shown in Fig. 30. It is evident the bigger gain parameter k_4 improves intensity of vibrations damping.

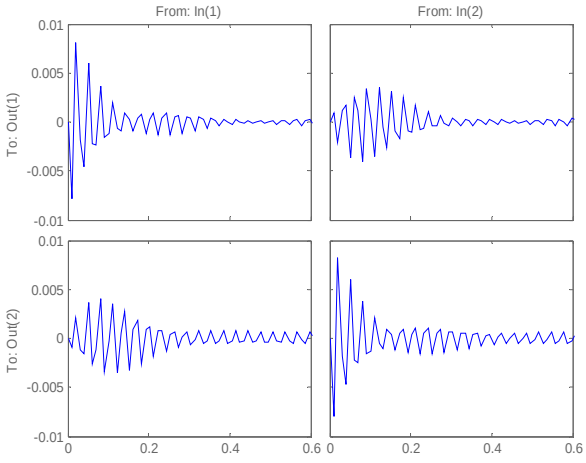

Fig. 30. The impulse response of closed-loop system for cross symmetric $\mathbf{K}_{r4}$ controller with gain k_4=1500 [1/s]

Now, we will check the stability of the system in full range of the considered angular speeds (from 0 to 300 [rad/s]). The real and imaginary parts of the roots of characteristic equation for closed-loop system with controller gain k_4=1500 [1/s] are shown in Fig. 31.

a)

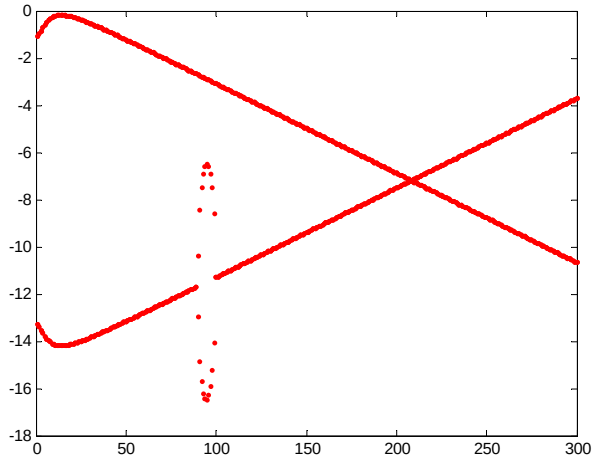

b)

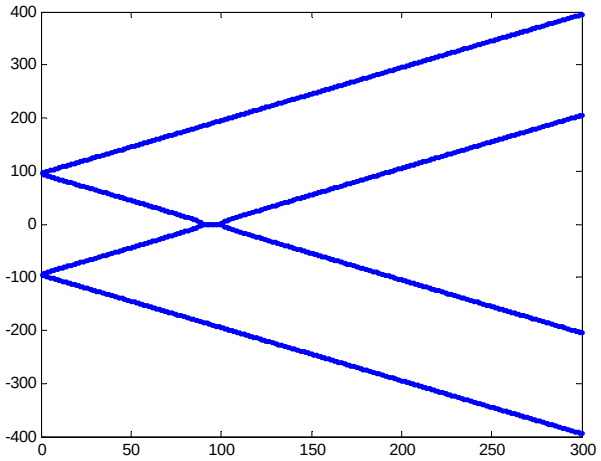

Fig. 31. Real (a) and imaginary (b) parts of the characteristic equation for gain k_4=1500 [1/s]

The closed-loop system is on the border of the stability for low rotor angular speeds (in the vicinity of 20 [rad/s]). It is appeared that there is upper limit on the value of the controller gain to stabilize the system in considered range of the rotor speeds. The upper limit is just k_4=1500 [1/s]. The lower limit of the controller gain was shown in Fig.28.

The gain matrix of controller (59) in the rotating coordinate system has the same two elements with opposite signs. The gain matrix of controller in non-rotating coordinate system has the form:

$$\mathbf{K}_4(s) = \mathbf{T}^T \mathbf{K}_{r4}(s)\mathbf{T} = \mathbf{K}_{r4}(s). \qquad (63)$$

The control laws in both coordinate systems - rotating and no rotating - are identical.

4.5. Comparison of control systems

To compare the different control systems we have taken into account the power consumption of power amplifiers which is the multiplication of control force and the velocity of the rotor vibrations. The most interesting are closed-loop systems with controllers $\mathbf{K}_{r2}$ i $\mathbf{K}_{r4}$. Thus, let us compare the power consumption by these control systems. In the case of $\mathbf{K}_{r2}$ controller the control force is proportional to rotational speed and in the second case of $\mathbf{K}_{r4}$ controller the control force is proportional to rotor displacement. The main rotor vibration movement is connected with angular speed Ω. Therefore, we assume that speeds v_x or v_y in motion directions are proportional to displacements in directions x or y and to angular speed Ω. Fig. 32 shows comparison of critical gain parameters for the $\mathbf{K}_{r2}$ i $\mathbf{K}_{r4}$ controllers. The $\mathbf{K}_{r4}$ closed-loop system is definitely the best one.

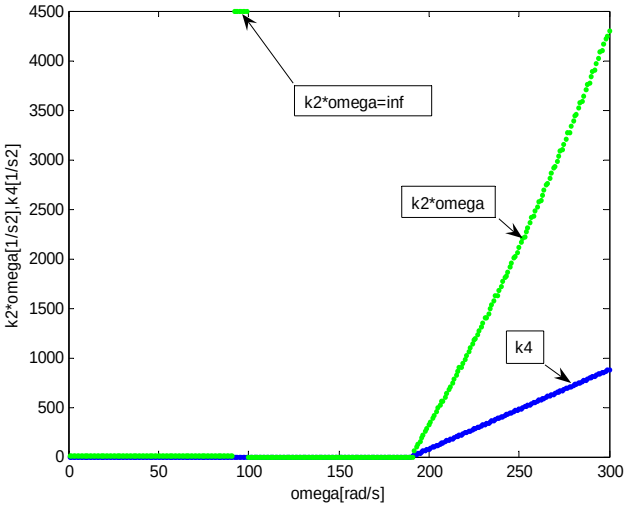

Fig. 32. The comparison of two critical gain parameters of control system

The closed-loop system with $\mathbf{K}_{r4}$ controller ensure the stability in full range of considered angular speeds. What more, for high rotational speeds the $\mathbf{K}_{r4}$ controller consume less power than others controllers. The $\mathbf{K}_{r4}$ controller has also good transient response (compare Figs 23 and 31).

5. CONTROL OF TORSIONAL/LATERAL ROTOR VIBRATIONS

Presently, the controller $\mathbf{K}_4$ will be joined to the full model of the rotor torsional/lateral vibrations. Its influence on the dynamic behaviour of the closed-loop system will be checked. The full rotor model with control of the lateral vibrations is presented in Fig.33.

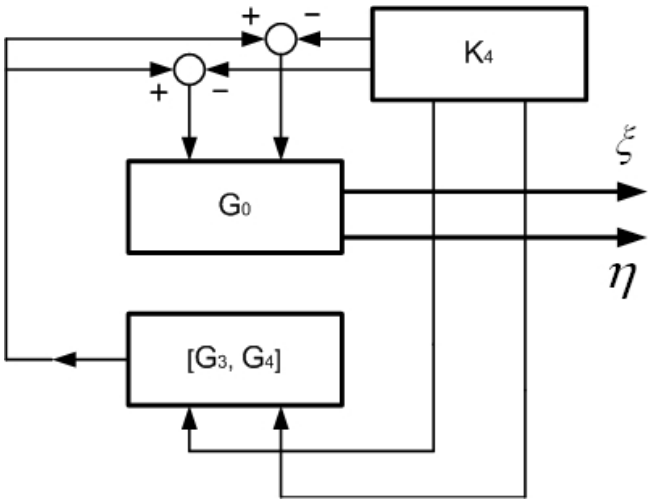

Fig. 33. Block scheme of the considered model for the rotor with active control of the lateral vibrations

To analyze the closed loop system the control forces defined as:

$$\mathbf{F}_r(s)=\begin{bmatrix} f_\xi(s) \\ f_\eta(s) \end{bmatrix} = -\begin{bmatrix} 0 & -k_4 \\ k_4 & 0 \end{bmatrix}\begin{bmatrix} \xi(s) \\ \eta(s) \end{bmatrix} + \begin{bmatrix} D(s) \\ F(s) \end{bmatrix}\phi(s).$$

The above input forces are introduced to the lateral vibrations model (21) to obtain the relations between the torsional and lateral vibrations in the closed loop system:

$$\frac{1}{D_{op}}\begin{bmatrix} D_{op}+Bk_4 & -A_2k_4 \\ A_1k_4 & D_{op}+Bk_4 \end{bmatrix}\begin{bmatrix} \xi \\ \eta \end{bmatrix} = \frac{1}{D_{op}}\begin{bmatrix} A_{2d} & B_d \\ -B_d & A_{1d} \end{bmatrix}\begin{bmatrix} D \\ F \end{bmatrix}\phi$$

Using above relation we can find the transfer functions between the lateral vibrations and torsional vibrations in the following form:

$$\begin{bmatrix} \xi \\ \eta \end{bmatrix} = \frac{1}{D_{op}D_{cl}}\begin{bmatrix} \left(D_{op}+Bk_4\right)\left(A_2D+BF\right)-A_1k_4\left(A_1F-BD\right) \\ A_2k_4\left(A_2D+BF\right)+\left(D_{op}+Bk_4\right)\left(A_1F-BD\right) \end{bmatrix}\phi$$

where D_{cl} is the characteristic polynomial of the closed-loop system (60) designed to control lateral vibrations:

$$D_{cl} = D_{op} + 2B_dk_4 + k_4^2.$$

In case of the minimal realization of the transfer functions the polynomial D_{op} from the denominator should be compensated by the same polynomial in the numerator. The above considerations lead to the reduced scheme (Fig. 34) were we have the following transfer functions:

$$G_{1c} = \frac{\left(D_{op}+Bk_4\right)\left(A_2D+BF\right)-A_1k_4\left(A_1F-BD\right)}{D_{op}D_{cl}},$$

$$G_{2c} = \frac{A_2k_4\left(A_2D+BF\right)+\left(D_{op}+Bk_4\right)\left(A_1F-BD\right)}{D_{op}D_{cl}}.$$

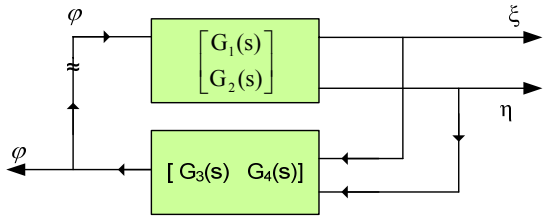

Fig. 34. Reduced block scheme of the closed-loop system with separated transfer functions of lateral and torsional vibrations.

The scheme from the Fig. 34 is very similar to the scheme from Fig. 7. Only the transfer functions $G_1(s)$, $G_2(s)$ was replaced by transfer functions $G_{1c}(s)$, $G_{2c}(s)$.
It means that full analysis of the system dynamics can be carried out according to procedure shown in Chapter 3.

6. SUMMARY

The full analysis of the rotor torsional/lateral vibrations is much simpler when we can divide the system into smaller subsystems. In this case the calculations are simplified
and we have deep insight into mechanisms leading to good or bed behaviour of the rotor motion. It is particularly important in the case of the rotor working in the wide range of the angular speeds. Turbo jet engines and flywheels are such rotors. For the vibration analysis the methods known from control theory was applied. In the paper it is Evans method. As well some other control methods can also be used to the vibration analysis.

The proposed approach was testified in the paper on the simple 3-mode rotor model (Jeffcott model). The torsional vibrations were separated from lateral vibrations and a feedback among subsystem was established. The subsystems are coupled by rotor unbalance and Evans method allows us show the critical values of the unbalance which destabilize rotor motion for different angular speeds. The lateral vibrations are stabilized by angular speed (rather gyroscopic effects proportional to the angular speed) and using again Evans method it is possible to find how big value of the rotor speed is sufficient to stabilize rotor motion.

Such analysis of the rotor vibrations appeared very useful for the choice of the control strategy. It indicated such control procedures which amplify the positive (stabilizing) mechanisms in the rotor dynamics. Such procedures can also lead to the energy saving control laws. In the case of lateral vibrations there were considered four control strategies. And these strategies were compared to indicate optimal one.

REFERENCES

1. **Ejkchoff P.** (1980), *Identyfikacja w układach dynamicznych*, PWN, Warszawa.
2. **Gosiewski Z.** (2008), Analysis of coupling mechanism in lateral/torsional rotor vibrations, *Journal of Theoretical and Applied Mechanics*, No. 4, Warsaw.
3. **Gosiewski Z., Muszyńska A.** (1992), *Dynamika maszyn wirnikowych* (*Dynamics of rotating machinery*), Publishing Office of WSInż. Koszalin.
4. **Juang J.-N**. (1994), *Applied System Identification*. Prentice-Hall Inc., (UK).
5. **Kaczorek T. (**1993), *Teoria sterowania i systemów* (*Theory of control and systems*), Wydawnictwo Naukowe PWN.
6. **Muszynska A., Goldman P., Bently D.E.** (1992), Torsional/lateral vibration cross-coupled responses due to shaft anisotropy: a new tool in shaft crack detection, *Conference of Institution of Mechanical Engineers*, Bath, Great Britain.
7. **Preumont A.** (2002), *Vibration Control of Active Structures: An Introduction*, Kluwer Academic Publishers, Dordrecht.
8. **Ulbrich H., Gunthner W.** (Editors) (2005), *Proc. IUTAM Symposium on Vibration Control of Nonlinear Mechanisms and Structures*. Munich, Germany. Springer, Dordrecht, the Netherlands.

The work is a part of project number PBZ-KBN-109/ T-10/2004 supported by State Committee for Scientific Research.